



Response to comments on

## Plastic deformation behavior and energy absorption performance of a composite metamaterial based on asymmetric auxetic lattices

César Garrido <sup>a,d</sup>, Gonzalo Pincheira <sup>b,\*</sup>, Rodrigo Valle <sup>c</sup>, Jorge Fernández <sup>d</sup>, Víctor Tuninetti <sup>e</sup><sup>a</sup> Master of Science in Engineering with a Major in Mechanical Engineering, University of Talca, Chile<sup>b</sup> Department of Industrial Technologies, University of Talca, Chile<sup>c</sup> PhD in engineering systems, Faculty of Engineering, University of Talca, Chile<sup>d</sup> Department of Mechanical Engineering, Universidad del Bío-Bío, Concepción, Chile<sup>e</sup> Department of Mechanical Engineering, Universidad de La Frontera, Chile

## ARTICLE INFO

## Keywords:

Composite metamaterial  
Auxetic Lattice  
Energy absorption  
Re-entrant structure  
Elasto-plastic behavior

## ABSTRACT

This study focuses on the design, behavior and experimental analysis of a novel metamaterial, consisting of an asymmetric auxetic three-dimensional structure (AATS) infused with polyester resin. Utilizing FDM additive printing, samples were created with customizable responses to compressive loads through varied design parameters. The objective is to surpass traditional material blending by enhancing stiffness and energy absorption. Striking a delicate balance, the AATS energy absorption properties are preserved while leveraging the stiffness of the resin. Despite its compact cubic form, not exceeding 27 mm on each side, this metamaterial showcases amplified characteristics, blending the AATS and polyester resin. The results hint at promising applications across military defense, automotive, aerospace sectors, and even potential replacements for articulated human skeletal components.

## 1. Introduction

Composite metamaterials in mechanics are the result of a combination of microstructures and different materials for specific property requirements. The continuous advancement of technology in the industrial world has led to constant new developments in materials and manufacturing [1]. Substantial improvements have paved the way for additive manufacturing (AM), enabling the production of components with complex geometries at various scales and in multiple materials [2]. A particular result of these advances are microstructured materials, also known as cellular structures [3], formed by struts and nodes rigidly interconnected through a periodic pattern [4]. Cellular structures become highly valuable for engineering design because their geometry can be manipulated to control the mechanical behavior of the macrostructure [5–7]. The topology of these structures is often designed and optimized based on the desired mechanical requirement [8,9], and in some cases even inspired by natural compounds such as wood, bone, or honeycomb [10–13]. The most frequently studied structures are sandwich panels [14] for applications in aerospace, marine and packaging industries [15] to excellent performance of light weight, sound insulation, high strength and high rigidity [16,17].

The geometrical freedom offered by AM may enable the creation of cellular structures with superior mechanical properties than traditional materials [18,19], e.g., high-strength/high-stiffness coupled

with low weight, and even structures that exhibit a negative Poisson's ratio [20–22]. The theoretical design of cell structures for tailored mechanical properties can be performed by analytical methods [8,23–25] together with tensile, compression, and bending experiments to assess and validate in plane [26–28] and out of plane [29,30] mechanical behavior. The appropriate geometric configuration to produce potentially high-performing cell structures [17,31], depends on the specific requirements. Strength and Young's modulus depend not only on the manufacturing material but also on a large extent on morphological parameters [32]. This is the case of honeycomb structures, one of the most studied structures and widely used in industrial applications, due to its attractive properties such as high rigidity and great impact resistance [33–35]. In Ref. [34], the mechanical behavior of a honeycomb structure is studied through FEM simulations and mechanical tests addressing geometric parameters, and the printing capacity of graded and hybrid networks with improved load-bearing capacities, useful for medical care and bioengineering, is demonstrated. In Ref. [36], a traditional honeycomb with triangular hierarchical substructures is proposed, where they analyze the compression behaviors in terms of stress and energy absorption. The results reveal that the hierarchical honeycomb design provides a high energy absorption capacity. In

\* Corresponding author.

E-mail address: [gpincheira@utalca.cl](mailto:gpincheira@utalca.cl) (G. Pincheira).<https://doi.org/10.1016/j.compstruct.2024.118410>

Received 11 March 2024; Received in revised form 12 May 2024; Accepted 18 July 2024

Available online 25 July 2024

0263-8223/© 2024 Elsevier Ltd. All rights reserved, including those for text and data mining, AI training, and similar technologies.

Ref. [37], a CCFR (continuous carbon fiber reinforced) composite honeycomb is proposed, and its performance under in-plane compression is presented. The analysis of experimental results of honeycombs with different materials demonstrates that carbon fiber not only improves the mechanical properties, but also changes the deformation characteristics of the structures. The literature is extensive and shows various studies on the enormous potential of these honeycomb structures, where researchers seek to improve the mechanical performance and many other characteristics such as their energy absorption capacity [38–42].

On the other hand, unlike the vast majority of materials that undergo transverse contraction when stretched, there are structures that expand laterally when subjected to tension, or contract laterally under uniaxial compression. These types of structures are known as auxetic because they experience a negative Poisson's ratio [43]. This auxetic effect produces attractive properties such as excellent resistance to indentation [44,45], high shear stiffness [45,46], remarkable fracture toughness [43] and unique acoustic energy absorption capabilities [47, 48]. A new class of accordion auxetic architecture with sinusoidal struts is proposed in Ref. [49], and is designed to improve the flat stretchability of cellular solids. These accordion-like sinusoidal architectures exhibit an improvement in the stretchability of cellular materials, even for those samples made from brittle polymers. Three types of double arrowhead-based 3D auxetic structures are proposed in Ref. [50], where the results indicate that 3D structures exhibit auxetic behavior with higher stiffness and can significantly improve quasistatic energy absorption performance compared to lattice networks for the same relative density. This auxetic structure based on the arrowhead configuration has been extensively studied in an analytical framework to predict in plane mechanical properties, including effective Young's modulus and Poisson's ratio [26,51]. On the other hand, the literature shows that the most promising auxetic cell is the auxetic structure with re-entrant struts due to the extraordinary ability to absorb energy with quasistatic and low velocity impact loads [43,52,53]. This structure has been widely studied, since the pioneering studies by Lakes 1987 [54], Wojciechowski 1987 [55], and Evans 1989 [56], where the first geometric configurations with re-entrant struts that exhibit an auxetic behavior are proposed, developing an analytical approach to microstructure to predict transverse expansion under a longitudinal load. In recent research, various theoretical design approaches have been employed to analyze the mechanical behavior of re-entrant struts. These approaches involve modeling the behavior using geometric parameters and manipulating Poisson's ratio and Young's modulus. The bending of these struts has been examined using Timoshenko's classical theory, which has proven to be effective in predicting the elastic properties of this structure. This model has provided valuable insights into the mechanical performance of re-entrant structures [18,57,58]. In addition, in Ref. [59], a new re-entrant structure is designed by adding wedge-shaped pieces to the conventional re-entrant structure. The additional piece not only regulates the structural stiffness during compression but also increases the stability of the structure by preventing lateral buckling of the structure, giving the metamaterial [60,61] more significant and stable auxetic behavior in compression. In Ref. [62], an auxetic honeycomb is proposed for a sandwich structure with a novel stepped design. The graduated auxetic design is achieved by varying the angle of the honeycomb cell through the thickness of the core. The results indicate that the reduction of the cell wall thickness to length ratio increases the bending failure stress and the specific energy absorbed by 35% and 45.8%, respectively. New reentrant auxetics with various substructures including equilateral triangles were built in Ref. [35]. The results show that the specific modulus increased by approximately 180%, the specific resistance increased by approximately 50%, and the specific energy absorption improved by approximately 160%. In Ref. [63], the novel design and performance improvement of the new re-entrant auxetic structures were presented and a comparative study of the uniaxial compression load behavior with regular honeycomb cells was performed.

**Table 1**

The results of the modulus of elasticity in the different printing directions according to the proposed design of the probe to know the properties of the material.

Position	Average MPa	Deviation standard MPa	Uncertainty (k=2)
Dy	1018.5	7.2	15.4
Dx	1085.2	15.6	25.3
Dz	2684.0	119.1	117.1

The new re-entrant structure showed better mechanical properties than the auxetic honeycomb structure, demonstrating higher compressive strength and higher energy absorption capacity than other structures. In Ref. [25,64,65] corrugated wall mechanical auxetic metamaterial with unique deformation mechanism is systematically studied. It has been found that the mechanical properties of the structure can be largely adjusted by simply increasing the wall thickness of the structure. The specific energy absorption of the proposed structure is significantly improved by employing continuous gradient and symmetric gradient design methods. In Ref. [66] new reinforced tubular structures with corrugated interior ribs and a gradient design method are proposed. The mechanical response, interaction effect and gradient effect of the proposed tubular structures are systematically studied through experimentation and numerical simulation. It has been found that tubular structures reinforced with corrugated inner ribs exhibit a progressive and stable deformation process under axial compression, achieving satisfactory specific energy absorption capacities of 27 J/g to 56 J/g.

Thus, the literature is extensive on the study of the great energy absorption capacity provided by this cellular structure [19,53,67–69]. However, most of the auxetic structures with re-entrant struts are designed symmetrically and with homogeneous mechanical properties in their three working directions. Therefore, different energy absorption behavior for each loading direction could be observed. In a previous study [70,71], a three-dimensional auxetic structure was proposed based on a known planar configuration that includes a design parameter called, hereafter  $\alpha$ , is responsible for the asymmetrical response. The experimental results reveal that the proposed structure can adequately provide different elastic properties in its three orthogonal directions. Furthermore, this auxetic cell influences the macrostructure to exhibit different stiffness behavior in three working directions.

This article is organized as follows: Section 2 describes the materials, auxetic design, manufacturing methods and testing of specimens. Section 3 presents the models applied for computing the mechanical performance of the auxetic structure and the composites metamaterial in the three orthogonal material directions. Section 4 provides the experimental results and the comparative analysis with modeling. Conclusions and future work are listed in Section 5.

## 2. Materials and methods

### 2.1. Additive manufactured polylactic acid for auxetic cells

Polylactic acid filaments (PLA) were used for printing auxetic structures and polyester resin was applied as the matrix to produce the composite metamaterial. Due to the well-known effect of printing orientation on resulting properties, specimens were prepared in the three main printing directions. Young's modulus and tensile parameters were determined in a Zwick/Roell machine with 2.5 kN load cell and using an extensometer, Fig. 1. The results of the material characterization are shown in Table 1.

The Young's modulus obtained from the material used in the fabrication of auxetic structures are subsequently required to determine the specific theoretical Young's modulus in each orthogonal direction for different angles by applying Timoshenko's model.

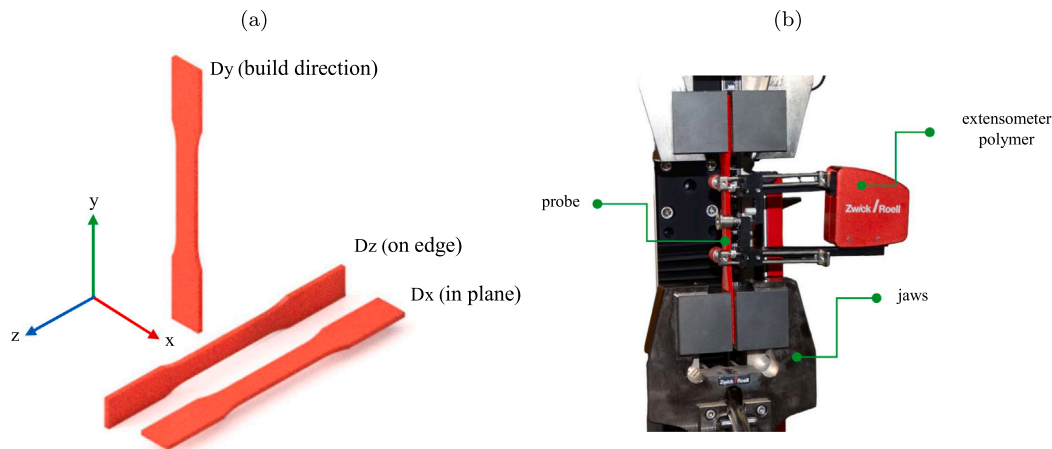


Fig. 1. (a) Schematic design of the printing directions (b) Characterization of Young's modulus with a polymer extensometer.

## 2.2. Polyester resin matrix

The polyester resin utilized in the experimental tests is characterized by its remarkable compression resistance properties, rendering it an excellent material for a wide range of applications. The resin's lightweight nature and cost-effectiveness contribute to its versatility in manufacturing processes, especially in applications where compression strength is a key factor. The representative values of the polyester resin used when comparing the contributions of its properties are as follows: an elastic modulus of 4.3 GPa, a compression strength of 60 MPa, and a maximum deformation of 0.08. These values are obtained experimentally after subjecting five resin specimens to tests with the same representative volume as the auxetic structure, with the aim of equalizing their contributions within the new material (auxetic structure polyester resin matrix). Furthermore, general data is provided, such as: orthophthalic resin, manual molding, translucent liquid resin, Brookfield viscosity 800 to 1400 cp, 2% cobalt octoate accelerator, reactivity time 6 to 14 min and its density of 1.1 g/cm<sup>3</sup>.

## 2.3. Design of auxetic lattice structure

In previous studies [57,72], symmetrical structures with auxetic behavior have been characterized. The structure model used is based into previous studies into the design and characterization of an asymmetric auxetic structure with an  $\alpha$  parameter that allows a contribution with a different behavior in its three directions, which has a differentiated behavior against a compressive load in its elastic zone [71]. This design parameter  $\alpha$  produces internal asymmetry in the structure, without altering the dimensions of the unit cell, as shown in Figs. 2 and 2(a). Since this structure has an orthotropic behavior,  $\alpha$  can take values  $0 < \alpha < 0.5$ . Since, for  $\alpha = 0.5$ , the traditional symmetric structure is obtained as a result. Otherwise, according to the applied Euler-Bernoulli approach, care must be taken that  $1/t^2 \ll L^2/t^4$  so that the structure is always dominated by the bending of its re-entrant struts. Thus, the design parameter should be  $\alpha > 2.5$ . For further details the reader is referred to [70,71].

The unit cell design studied, has dimensions of its elements appropriate for printing by FDM additive printing with an average size of 27 mm square and a mass of 6.788 g and a volume of 6.777 mm<sup>3</sup>. The digital model was worked on in the Autodesk Fusion 360 program and was later exported to STL format. The dimensions of the unit cell are indicated in Fig. 3, considering the  $\alpha$  variant within the values of 0.27, 0.33 and 0.40, which differentiates of structures to be studied and characterized in the area of elastoplastic behavior. This  $\alpha$  factor enables control of the degree of asymmetry of the structure as shown in Figs. 3 and 2. Auxetic structure designs shown in Fig. 4 is composed of

$3 \times 3 \times 2$  unit cells (18-unit cells) the justification for the configuration of the number of cells, according to experiences from previous tests where the capacity of the machine was not capable of bringing the structure to the level of failure. Three specimens by each cartesian axis and  $\alpha$  condition were tested, with a total of 27 specimens for unfilled structures and 27 specimens for resin filled structures. The machine used in the experimentation is stated in a later chapter. The machine used in the experimentation is stated in a later chapter. The final dimensions obtained is a cube with 27 mm edge. The auxetic structures were manufactured by FDM (fused deposition modeling) on an Artillery Genius Pro printer and using PLA filament. The pre-processing was carried out with the Cura program, with a layer height of 0.2 mm, print nozzle diameter 0.4 mm, print infill 100%, printing speed of 55 mm/s, the nozzle heated to 210 °C, and a bed temperature of 60 °C. It is important to highlight that the manufacture of all the elements that contained resin alone or resin plus structure were manufactured with the same configuration of accelerator and resin activator. This mean that their characteristics are not affected by the resin preparation and at the same time, thereby ensuring the drying condition of the elements, which would later be characterized by means of a compression test.

The polyester resin was prepared at the same time that the structures were filled with the resin. Furthermore, the dimensions obtained from the resin cube are directly related to the volume used for filling the cellular structure. This allows the strength properties to be evaluated based on the same amount of material.

Finally, cubic specimens with the same previous geometry were prepared only with polyester resin, in the same way, resin-filled auxetic structures

## 2.4. Experimental testing

The mechanical behavior of resin, auxetic structures and auxetic composite samples has been investigated through compressive tests. A Zwick/Roell model Z100 tensile machine with a 100 kN load cell was used. The strain rate applies was 0.001/s, corresponding to a displacement speed of the plate of 1.0 mm/min according to the ASTM D1621 standard. Strain was calculated using crosshead displacement. First, the auxetic structures were characterized in their three orthogonal directions and with different factors  $\alpha$  (0.27; 0.33 and 0.40). Second, pure polyester resin specimens were studied. Finally, auxetic structure resin-filled were characterized in their three orthogonal directions with different factors  $\alpha$  (see Fig. 5).

The assembly of the individual structures as well as the assembly of the structures with resin must be carried out according to the measurement of their properties on their different orthogonal axes as shown in Fig. 6

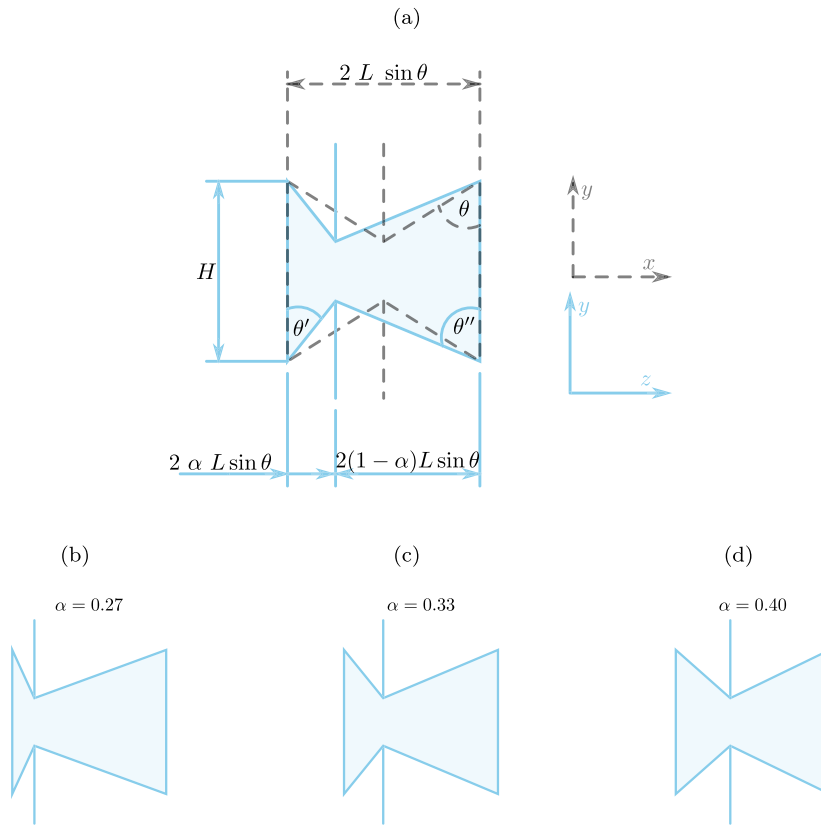


Fig. 2. (a) Representation of asymmetry generated by the design parameter  $\alpha$  in its different orthogonal directions. (b), (c) and (d) Schematic representation of the effects of the  $\alpha$  variable on the shape of unit cells. The higher the parameter  $\alpha$ , the lower its degree of asymmetry.

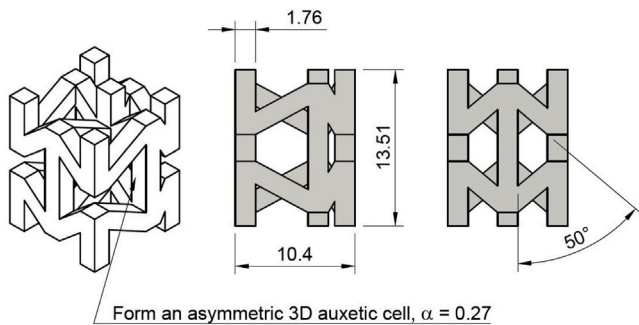


Fig. 3. Dimensions of the unit cells in their most relevant elements.

### 3. Modeling the elasto-plastic behavior

#### 3.1. Elastic response

The elastic behavior of re-entrant structures can be modeled accurately through Timoshenko's classic theory [57,73]. The re-entrant structure is modeled based on its design parameters: the vertical length of the cell  $H$ , the length of the re-entrant struts  $L$ , the re-entrant angle  $\theta$  and the thickness of the cross-section  $t$ . Therefore, our previous work [70,71] showed that this theory also makes it possible to model this structure with an asymmetry pattern through a new design parameter  $\alpha$ . Furthermore, this theoretical model has been shown to predict very successfully a new re-entrant structure modified with a rotation angle of its struts to obtain an orthotropic behavior [74]. Eqs. (1)–(3) are applied to model the Young's modulus of this orthotropic structure

for each orthogonal direction.

$$E_x = \frac{2t^4}{L^3 H \cos^2 \theta} E_s \quad (1)$$

$$(E_z)_i = \frac{\sigma t^4 \sin \theta^*}{F_i (L^*)^2 \cos^2 \theta^*} E_s \quad (2)$$

$$(E_y)_i = \frac{\sigma t^4 (\frac{H}{L^*} - \cos \theta^*)}{F_i (L^*)^2 \sin^2 \theta^*} E_s \quad (3)$$

where the geometric parameters  $\theta^* = \{\theta, \theta', \theta''\}$  and  $L^* = \{L, L', L''\}$  as appropriate to the re-entrant strut type  $i$ , which depends on the layout parameter  $\alpha$ , and  $E_s$  is the Young's modulus of the manufacturing material. For further details, the reader is referred to [70,71] where this model has been studied in depth.

#### 3.2. Stress strain modeling under plasticity

The energy absorption capacity of auxetic structures under plastic deformation should potentially be improved in structures with a negative Poisson's ratio as indicated by the literature [75–77]. As a consequence of utilizing an auxetic structure, it can be stated that the energy absorption condition was established between the final stage of elastic behavior and the onset of the zone called densification. This zone is referred to as the energy absorption plateau region. The plateau region is found in the force or stress response following the yielding point of an energy-absorbing structure. This region is characterized by a relatively constant or near-constant force or stress, and a gradually increasing deformation. In this region, the energy-absorbing structure dissipates the maximum amount of energy possible without significantly increasing the force or stress. This is why the plateau region is a critical part of the response curve of an energy-absorbing structure, as it ensures effective and safe energy dissipation. The expression applied

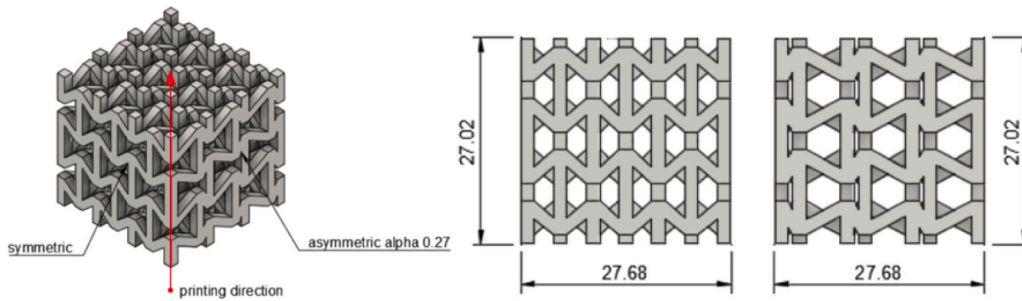


Fig. 4. Dimensions of the cellular structure with a conformation of three-unit cells on its vertical axis and horizontal axis.

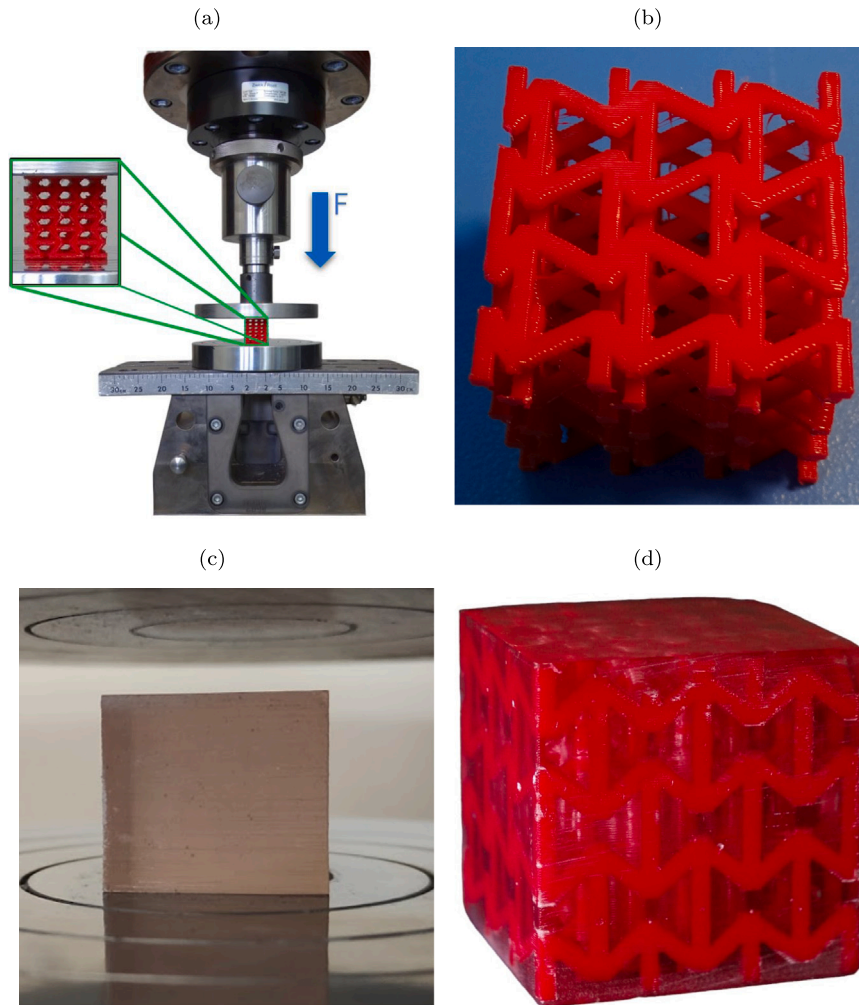


Fig. 5. (a) Compression test (b) auxetic structure, (c) solid polyester resin, (d) auxetic structure filled with polyester resin.

to estimate the engineering stress is derived from the energy per unit volume as shown in Eq. (4).

$$\sigma_p = \frac{W_p}{\Delta_e} = \int_{\epsilon_y}^{\epsilon_d} \sigma(\epsilon) d\epsilon \quad (4)$$

where the  $(\sigma_p)$ , represents the area under the stress curve between the points  $(\epsilon_y)$  and  $(\epsilon_d)$ . To determine the starting point  $(\epsilon_y)$  of the energy absorption zone, the criterion of considering the beginning as the point where the zone of elastic proportional behavior of the structure or resin-filled structure ends is used. For the end, it is established when, after a significant advance on the horizontal response of the structure or called the energy absorption zone, there is a noticeable change in the horizontal trend of the stress towards an abrupt vertical

trend (accelerated stress increase). Significantly and the deformation decreases, it is at this point where a vertical reference line is plotted that establishes the end of the energy absorption zone  $(\epsilon_d)$ . Determining the beginning and end of the energy absorption zone in the tests conducted on the structure without resin proved to be considerably intricate. This complexity arose from the fragile nature of the structure and the manufacturing process used (FDM), which led to the fracture of its struts subsequent to an increase in compression levels induced by the bending stress experienced by the main struts. Now, in the case of the resin-filled structure, this condition was less difficult due to the uniformity of its behavior when a polyester resin was added to the structure in all its interior cavities, which considerably improved its resistance against shear force in the struts.

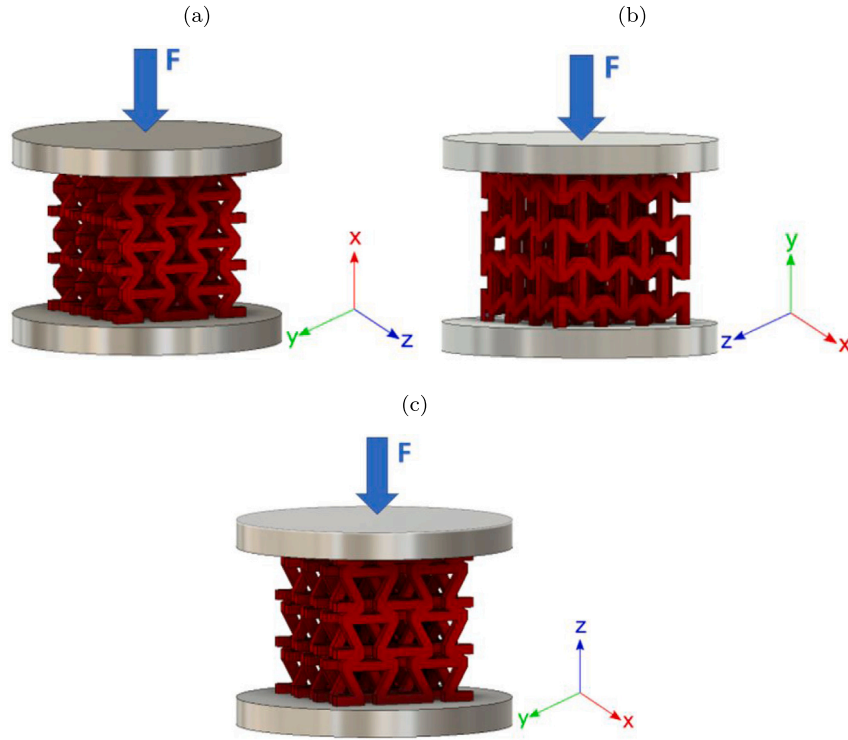


Fig. 6. This shows the positioning of the structures in the compression plates, where (a) represents the x-axis direction, (b) the y-axis direction (printing direction in the FDM process), and (c) the z-axis direction.

In the elastic zone, the Young's modulus in the orthogonal axes for different  $\alpha$ -values (0.27;0.33;0.40) of structures without resin is computed for establishing the level of elastic orthotropy Eq. (5) [78]:

$$I_{E \text{ direction}} = \sqrt{\frac{(E_x - E_{\text{direction}})^2 + (E_y - E_{\text{direction}})^2 + (E_z - E_{\text{direction}})^2}{E_{\text{direction}}}} \quad (5)$$

where  $E_x, E_y, E_z$  represents the Young's modulus for each particular orthogonal direction of the structure and assuming an  $\alpha$  value also defined for each analysis.

The orthotropic coefficient ( $I_{E \text{ direction}}$ ) for each axis is a function of  $\alpha$ -value. However, to determine a representative value of the structure, the dimensionless number of orthotropy index ( $I_E$ ) is defined as given in Eq. (6):

$$I_E = \text{Max}E_{x,y,z} - \text{Min}E_{x,y,z} \quad (6)$$

where ( $\text{Max}E_{x,y,z}$ ) represents the maximum value found for Young's modulus with a given  $\alpha$  for each orthogonal axis and ( $\text{Min}E_{x,y,z}$ ) the minimum found for the same  $\alpha$  condition.

This coefficient represents the orthotropy of the structure, which is affected mainly by the Young's modulus in the different orthogonal axes. The resulted value is determined by the maximum difference interval between the highest value found and the lowest value found according to each direction. The functionality of the characterized structures is based on their combination of auxetic structures and resin, which has an orthotropic behavior in its different axes (x, y, z). Consequently, it is necessary to identify their orthotropy levels in each orthogonal direction [78], which is why the ratio of energy absorption level in the plateau zone for each working direction is used as an input variable. The responses of the different structures with  $\alpha$  value variations show differentiated behavior when subjected to a combination of stresses in the orthogonal material directions. An anisotropy coefficient expression is applied for the condition of different  $\alpha$ , taking as input the average stress values of the structure in different directions for a given  $\alpha$  Eqs. (7) and (8).

$$I_{\sigma \text{ direction}} = \sqrt{\frac{(\sigma_x - \sigma_{\text{direction}})^2 + (\sigma_y - \sigma_{\text{direction}})^2 + (\sigma_z - \sigma_{\text{direction}})^2}{\sigma_{\text{direction}}}} \quad (7)$$

$$I_{\sigma} = \text{Max}\sigma_{x,y,z} - \text{Min}\sigma_{x,y,z} \quad (8)$$

( $I_{\text{direction}}$ ) represents the orthotropic coefficient measured in a specific direction. ( $\sigma_x$ ), ( $\sigma_y$ ) and ( $\sigma_z$ ) represent the stress (area under the curve); and ( $I_{\sigma}$ ) is the orthotropic coefficient that specifies the deviation of work from its transverse directions.

#### 4. Results and discussion

To determine the mechanical behavior of this asymmetric auxetic structure reinforced with polyester resin, multiple quasistatic compression experiments were carried out until rupture. From previous studies [70,79], the asymmetric auxetic structure exhibited orthotropic behavior when the  $\alpha$  design parameter decreases. Therefore, it is expected that this mechanical behavior can also be exhibited in the plastic zone, particularly in the energy absorption capacity. However, the study of energy absorption on this auxetic structure manufactured with FDM technology has been difficult because the nature of the layer by layer process reduces the ductility of the plastic zone. For this reason, an isotropic matrix was incorporated as reinforcement to increase the deformation capacity in the plastic zone. Therefore, to demonstrate the mechanical contribution of each component, preliminary quasistatic compression experiments were carried out on the auxetic structure manufactured with PLA, a sample of polyester resin and finally the combination of both materials, as shown in Fig. 7.

The results show that the auxetic structure by itself has low resistance; however, it can experience plastic deformations of up to 45%. While the polyester resin sample demonstrate higher mechanical resistance, its ability to experience plastic deformation is less 10%. On the other hand, the resulting auxetic structure reinforced with polyester resin provides higher mechanical resistance and also large deformations. These preliminary results show that the contribution of the polyester resin enables an increase in the mechanical resistance of the structure and also increases the capacity of plastic deformation. Therefore, the new created structure possess an improved energy

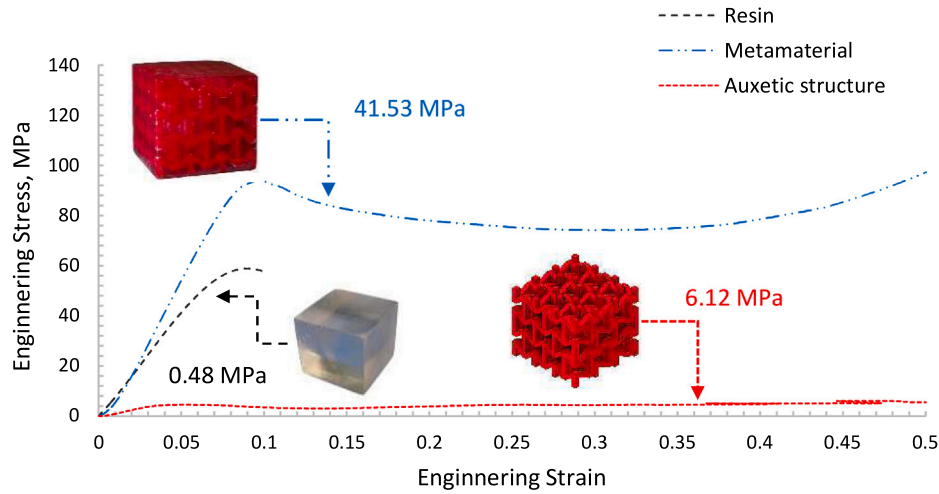


Fig. 7. Compressive experimental stress–strain behavior of the auxetic structure, the resin and the composite auxetic metamaterial. Stresses shown in the graph are computed applying the energy criteria and Eq. (4).

**Table 2**  
Plateau stress and specific energy absorption (SEA) of the: resin, structure and metamaterial.

Description	$\alpha$	Axis	Density (g/cm <sup>3</sup> )	Stress plateau (MPa)	SEA (J/g)
Metamaterial	0.27	z	1.32	37.99	28.76
		y		35.53	26.90
		x		41.53	31.44
	0.33	z	35.81	27.11	
		y	37.27	28.21	
		x	37.87	28.67	
0.40	z	33.18	25.12		
	y	35.00	26.50		
	x	34.69	26.26		
Structure	0.27	z	1.24	3.74	3.02
		y		4.14	3.34
		x		6.12	4.94
	0.33	z	1.00	0.81	
		y	1.80	1.45	
		x	3.09	2.49	
	0.40	z	1.55	1.25	
		y	0.98	0.79	
		x	1.81	1.46	
Resin	–	–	1.10	0.48	0.44

absorption capacity. In addition, owing to the asymmetry pattern of the auxetic structure, it is to be expected that the energy absorption capacity will be different for each load direction. Thus, the following section shows the experimental results of the auxetic structures made with PLA and the structures reinforced with polyester resin, where the specific energy absorption capacity for each case is analyzed. Table 2 shows the quantitative, applying Eqs. (4) and (9) [25].

$$SEA(\epsilon) = \frac{\int_{\epsilon_d}^{\epsilon_y} \sigma(\epsilon) d\epsilon}{\rho} \quad (9)$$

where  $SEA(\epsilon)$  is the specific energy absorption, ( $\rho$ ) the specific density of the characterized element, ( $\sigma$ ) the plateau stress between two engineering strain points ( $\epsilon_y$ ) and ( $\epsilon_d$ ).

#### 4.1. Elastic deformation of auxetic structure

The results obtained experimentally under quasistatic compression up to the elastic zone limit are analyzed. Therefore, considering that the internal geometry of the structure provides an orthotropic behavior,

energy absorption at different levels in its three orthogonal axes are expected, as shown in Fig. 6. To validate this orthotropic behavior with this combination of geometric parameters, the Young’s modulus of this structure is first analyzed similarly to previous studies [70,71, 74]. The results were determined according to experimental tests in a strain level between 0.00 and 0.03 mm/mm in a linear zone. Fig. 8 illustrates stress–strain curves for  $\alpha = \{0.27; 0.33; 0.40\}$ ; the influence of  $\alpha$  on the material orthotropy is evident as the  $\alpha$  value is lower (more asymmetric). The smaller the design parameter  $\alpha$ , the internal asymmetry of the structure increases. Therefore, the difference between the elasticity moduli  $E_x$  and  $E_z$  increases. On the other hand, the smaller the design parameter  $\alpha$ , the elasticity modulus  $E_y$  increases, due to the asymmetric distribution of the internal loads. As established in a previous work [70,71].

Fig. 9 compares theoretical and experimental Young’s modulus results for the main work directions and factor  $\alpha$ . It corroborates the greater orthotropy at lower factor  $\alpha$  and also validates the theoretical model used in comparison with experimental results.

The experimental results for Young’s modulus agree quite well with Timoshenko’s theory in every case, with an average error of around 0.5%. In addition, the results obtained for Young’s modulus confirm that the lower the  $\alpha$  design parameter, the higher the orthotropic coefficient. This is evident through Eq. (5) the level of orthotropy for each structure can be quantified. In this way, the structure  $\alpha = 0.27$  has an orthotropy coefficient  $I_E = 0.14$ , while  $\alpha = 0.33$  has  $I_E = 0.05$  and finally  $\alpha = 0.40$  has  $I_E = 0.04$ . Which indicates the deviation among the experimentally measured Young’s modulus for each structure. Where the Young’s modulus  $x$ ,  $y$ , and  $z$  have a greater difference among them. Therefore, it is expected that this orthotropic behavior within the elastic zone will change and be reflected in the energy absorption capacity.

On the other hand, Fig. 12 shows the experimental stress vs. elastoplastic strain curves for the auxetic structures. To evaluate the influence of the asymmetry pattern on the energy absorption capacity, the experimentation was carried out under different configurations of the design parameter  $\alpha = \{0.27; 0.33; 0.40\}$ . The energy absorption capacity of the auxetic structures was measured by loads and deformations, using the testing machine’s load and displacement recording devices. It is important to note that the energy absorption measured in MPa is indicated under each experiment curve. In addition, the range of deformations in which it was measured is indicated.

Undoubtedly, the results obtained confirm our hypothesis. As can be seen in the graphs, the asymmetrical pattern produces different energy absorption capacities in the three load directions for each structure.

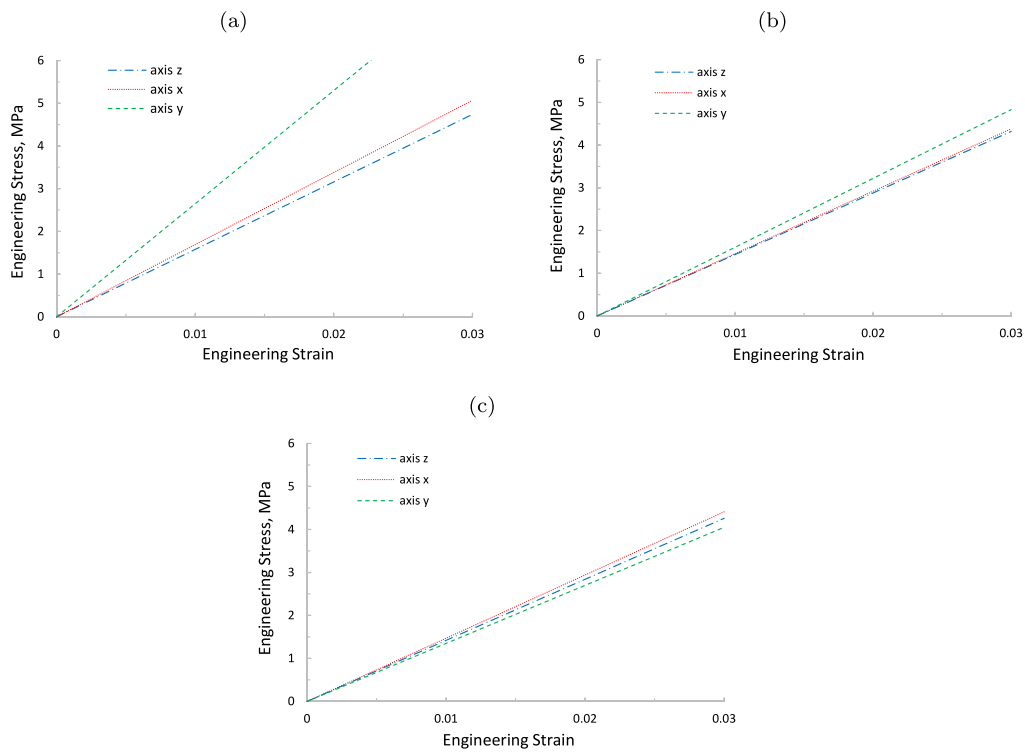


Fig. 8. Experimental engineering stress vs. strain for each auxetic structure reinforced with polyester resin in its three orthogonal directions and for each asymmetry pattern: (a)  $\alpha = 0.27$ ; (b)  $\alpha = 0.33$ ; and (c)  $\alpha = 0.40$ .

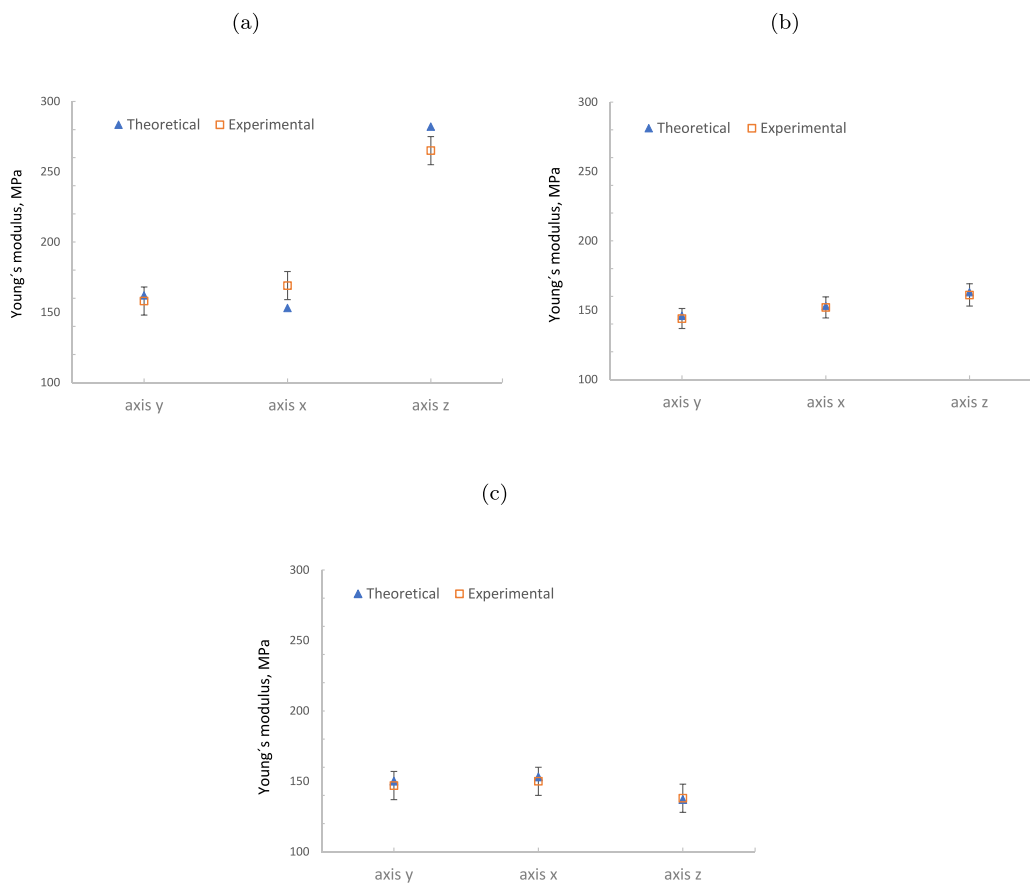


Fig. 9. Comparison of theoretical vs. experimental Young's modulus for different levels of asymmetry: (a)  $\alpha = 0.27$ ; (b)  $\alpha = 0.33$ ; and (c)  $\alpha = 0.40$ .

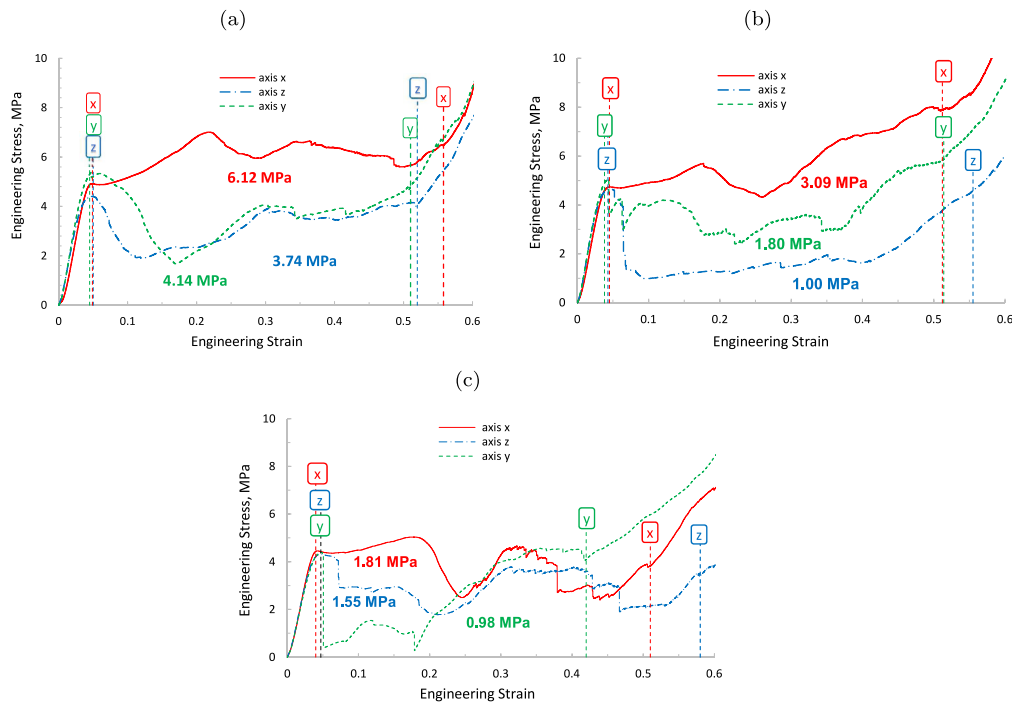


Fig. 10. Experimental results of engineering stress vs. strain for each auxetic structure in its three orthogonal directions and for each asymmetry pattern (a)  $\alpha = 0.27$ ; (b)  $\alpha = 0.33$ ; and (c)  $\alpha = 0.40$ .

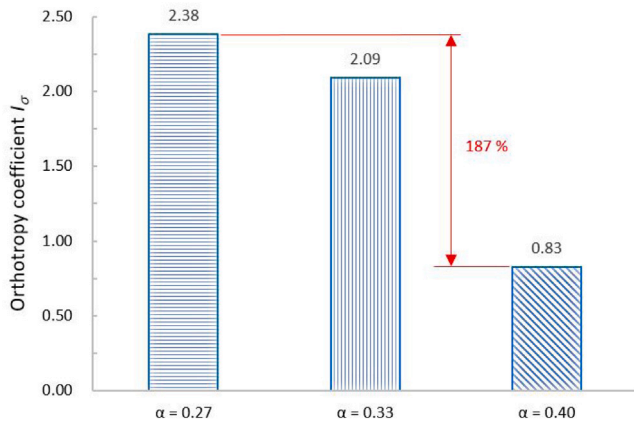


Fig. 11. Orthotropic behavior of the structure quantified with its stress under the curve in its three orthogonal directions and for each asymmetry pattern  $\alpha = \{0.27; 0.33; 0.40\}$ .

The smaller the design parameter  $\alpha = 0.27$ , the greater the difference between the energy absorption capacity under compression in the  $x$ ,  $y$ , and  $z$  directions. This opens up great possibilities in engineering applications, where a differentiated mechanical behavior is required for each direction of work. Fig. 11 shows the level of plastic orthotropy according to the applied Eq. (8), for the behavior of the structure on its different orthogonal axes for each different  $\alpha$ . In comparison to an  $\alpha = 0.40$ , the  $\alpha = 0.27$  condition displays percentage terms up to 187%, demonstrating that the  $\alpha$  design parameter has a higher degree of orthotropy between its orthogonal axes.

Furthermore, a novel finding from this experiment requiring analysis is that, in most cases, the energy absorption capacity increases by around 94% with a smaller  $\alpha$  design value. Therefore, only by modifying the asymmetry pattern is it possible to double or triple the energy absorption capacity in its three orthogonal directions. However, the plastic zone of the structures also exhibits highly erratic behavior due to the layer by layer interface provided by the FDM manufacturing

process, which causes the struts to break randomly under flexion [80, 81]. This prevents this structure from taking advantage of its great energy absorption attribute. Hence, it is necessary to have selective laser sintering technologies, and thus studying this property poses a challenge [82]. However, to provide greater resistance, the auxetic structures have been reinforced with polyester resin to improve their plastic behavior. The next section shows the results.

#### 4.2. Energy absorption of auxetic composite metamaterial

In this section, the experimental results obtained for the auxetic structure reinforced with polyester resin under quasistatic compression until rupture are analyzed. Considering our preliminary experiments indicated in Fig. 10, it is expected that high mechanical resistance and large plastic deformations will be obtained as a result, as a combination of the two materials. Fig. 12 shows the experimental curves of engineering stress vs. strain for Auxetic structures reinforced with polyester resin and for different patterns of asymmetry  $\alpha = \{0.27; 0.33; 0.40\}$ . It is important to mention that the graph indicates the range of deformations in which the energy absorption was measured. However, due to the great resistant capacity of the structure, the test could not be completed, since the limit of the capacity of the testing machine was reached. For this reason, the measurement range is considered from when the yield stress is exceeded to the end of the curve because a clear point of inflection is not observed in the curve in which the stress tends to infinity. In this way, the energy absorption measured in MPa is indicated under each experiment curve.

The results show that the structures reinforced with polyester resin increased their yield strength around fourteen times compared to the auxetic structure without reinforcement indicated in Fig. 12 while the energy absorption capacity increases more than twenty in some cases. On the other hand, thanks to the polyester resin reinforcement, the mechanical behavior in the plastic area is no longer random and becomes more homogeneous. However, its orthotropic behavior continues to be dependent on  $\alpha$ . It is evident that the auxetic structure continues to contribute with the pattern of asymmetry given that the energy absorption in structures with asymmetry pattern  $\alpha = 0.40$

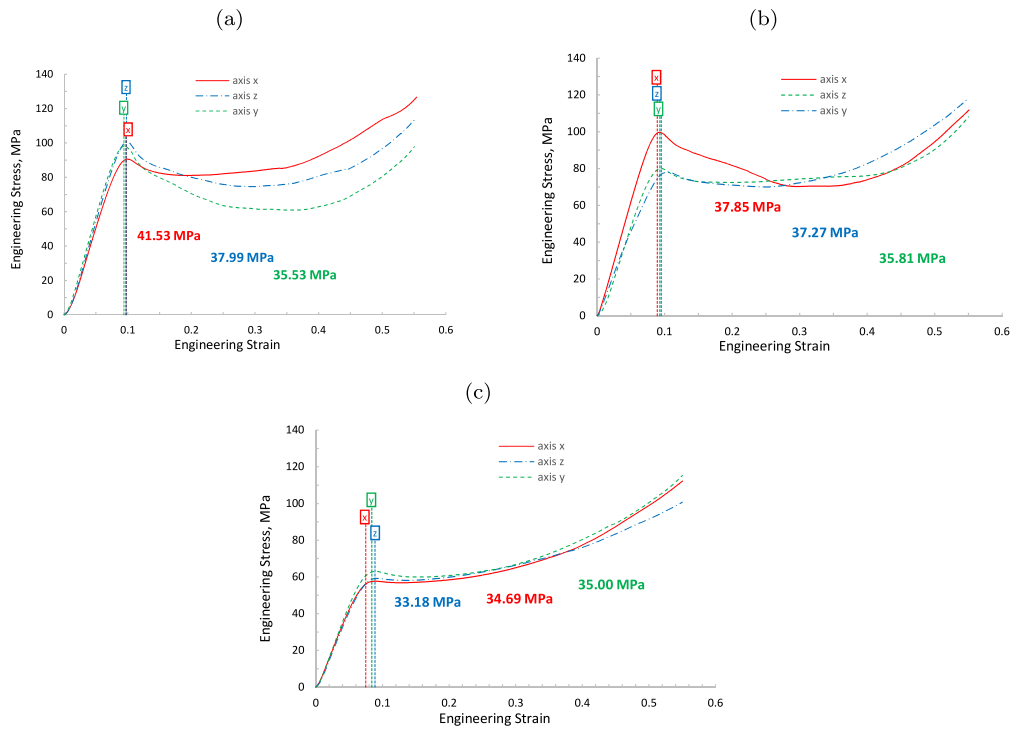


Fig. 12. Experimental engineering stress vs. strain for each auxetic structure reinforced with polyester resin in its three orthogonal directions and for each asymmetry pattern (a)  $\alpha = 0.27$ ; (b)  $\alpha = 0.33$ ; and (c)  $\alpha = 0.40$ .

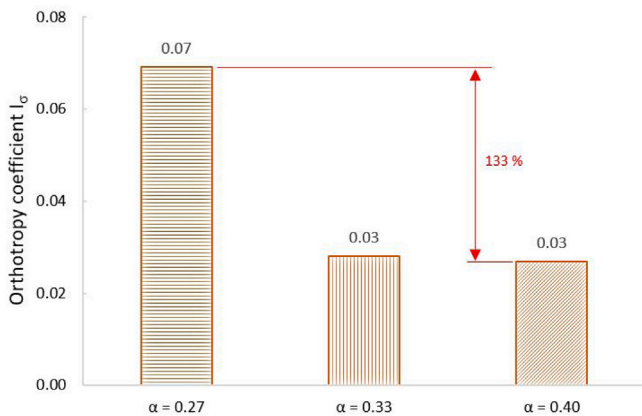


Fig. 13. Orthotropic behavior of the structure filled with polyester resin quantified with its stress under the curve in its three orthogonal directions and for each asymmetry pattern  $\alpha = 0.27$ ;  $\alpha = 0.33$ ; and  $\alpha = 0.40$ .

under compression in  $x$ ,  $y$ , and  $z$  directions are very similar to each other. As the pattern of asymmetry becomes smaller the difference in energy absorption between the  $x$ ,  $y$ , and  $z$  directions becomes larger. Thus, the orthotropy increases as the design parameter  $\alpha$  decreases. This behavior can be clearly seen in Fig. 13, where the orthotropic coefficient calculated with Eq. (8) is represented graphically through the energy absorbed in each direction.

Through this coefficient, the anisotropic behavior in the plastic zone of the structure in terms of energy absorption can be quantified. This confirms that the smaller the value of the design parameter  $\alpha$ , the greater the anisotropy of the structure. However, the anisotropy achieved in the plastic zone is lower than that obtained by the auxetic structure without resin. This is because, in this case, it has been reinforced with an isotropic matrix. However, it is important to note

that the levels of anisotropy in the plastic zone could have been higher, considering that the structures did not break due to the maximum capacity of the testing machine. On the other hand, it can be seen that only by modifying the design parameter  $\alpha$  can energy absorption be manipulated. An average 6.0% increase in energy absorption can be observed with a smaller parameter  $\alpha$ . In the previous case, the auxetic structure experienced a much greater increase in energy absorption. However, in this case, the increase in energy is reduced due to the incorporation of an isotropic reinforcement matrix.

The results of this research provide the development of a new composite metamaterial of an auxetic structure reinforced with a resin matrix to increase its mechanical performance. Thanks to the asymmetric pattern resulted from auxetic structure, the new material provides different levels of orthotropy. In addition, the reinforcing resin matrix highly increase the material levels of energy absorption differentiated on its three orthogonal axes. In future works, we will study the effect of different resin matrices as reinforcement to maximize the energy absorption performance of the structure. This offers great potential in applications where a differentiated mechanical behavior is required, as in the case of a prosthetic foot, wearable devices, and impact resistance aerospace components.

### 5. Conclusions

This work reports the experimental responses of a modified auxetic structure with different behaviors on their respective orthogonal axes. In addition, a new composite metamaterial is investigated using a reinforced resin matrix for the auxetic structure. A relevant conceptual idea that emerges from the study is that the reinforcement can be designed according to the new material. The results indicated that the orthotropic levels of the auxetic structure were not significantly affected by the addition of polyester resin. The strength levels, energy absorption and orthotropy coefficient of the new metamaterial are shown below.

1. The orthotropic index levels characterized by the Young's moduli are proven to differ by 70% with respect to  $\alpha = 0.27$  vs. an  $\alpha = 0.40$ . This confirms that the lower the  $\alpha$  value, the higher the level of orthotropy between the orthogonal axes.
2. Regarding the energy absorption capacity of the structure in terms of stress, a significant difference is found for various asymmetric cell  $\alpha$  values. The maximum stress difference is 70% for the z-axis, 76% for y-axis, and 59% for x-axis.
3. Polyester resin incorporated as a matrix reinforcement to the auxetic structure effectively increases the resistance behavior. The maximum strength of 4.3 MPa for the asymmetric structure with  $\alpha = 0.27$ , algebraically added to the individual resin strength of 56 MPa, gives an expected strength value of 60.3 MPa. However, this strength is exceeded by the 93 MPa provided by the metamaterial structure. Therefore, an attractive 35% increase in expected strength is achieved by combining the two components.
4. The specific energy absorption level of the auxetic structure characterized by 1.45 J/g algebraically added to the polyester resin of 3.04 J/g gives 4.49 J/g. Therefore, the 31.4 J/g of the auxetic composite metamaterial surpasses by 83% the expected value of specific energy absorption.

Design of the investigated auxetic structures can be adapted from the variation of the  $\alpha$  design parameter according to the response levels in different orthogonal axes. Additionally, the overall dimensions of the structure remain unaltered in terms of height, width, and length. This mechanical features are essential for adapting material and structures in different industrial applications such as building engineering, automotive, aeronautical and aerospace. Current work is focused on personal protection elements to aid in the care or protection of the lives of children and adults against incidents with high energy impacts.

## Funding

This work was funded by the National Agency for Research and Development (ANID) Beca de Doctorado Nacional 21191100 and Fondecyt Regular project 1241729.

## CRediT authorship contribution statement

**César Garrido:** Writing – review & editing, Writing – original draft, Methodology, Investigation, Conceptualization. **Gonzalo Pincheira:** Writing – review & editing, Writing – original draft, Supervision, Methodology. **Rodrigo Valle:** Writing – review & editing, Methodology, Data curation, Conceptualization. **Jorge Fernández:** Writing – review & editing, Methodology. **Victor Tuninetti:** Writing – review & editing, Writing – original draft, Supervision.

## Declaration of competing interest

The authors declare the following financial interests/personal relationships which may be considered as potential competing interests: Gonzalo Pincheira Orellana reports was provided by University of Talca. If there are other authors, they declare that they have no known competing financial interests or personal relationships that could have appeared to influence the work reported in this paper.

## Data availability

Data will be made available on request.

## References

- [1] du Plessis A, Razavi SMJ, Benedetti M, Murchio S, Leary M, Watson M, Bhatte D, Berto F. Properties and applications of additively manufactured metallic cellular materials: A review. *Prog Mater Sci* 2022;125:100918. <http://dx.doi.org/10.1016/j.pmatsci.2021.100918>, URL <https://www.sciencedirect.com/science/article/pii/S0079642521001420>.
- [2] Magliaro J, Altenhof W, Alpas AT. A review of advanced materials, structures and deformation modes for adaptive energy dissipation and structural crashworthiness. *Thin-Walled Struct* 2022;180:109808. <http://dx.doi.org/10.1016/j.tws.2022.109808>, URL <https://www.sciencedirect.com/science/article/pii/S0263823122005018>.
- [3] Korkmaz ME, Gupta MK, Robak G, Moj K, Krolczyk GM, Kuntoğlu M. Development of lattice structure with selective laser melting process: A state of the art on properties, future trends and challenges. *J Manuf Process* 2022;81:1040–63. <http://dx.doi.org/10.1016/j.jmapro.2022.07.051>, URL <https://www.sciencedirect.com/science/article/pii/S1526612522005199>.
- [4] Estakhrihaghghi E, Mirabolghasemi A, Shi J, Lessard L, Akbarzadeh A. Architected cellular fiber-reinforced composite. *Composites B* 2022;238:109894. <http://dx.doi.org/10.1016/j.compositesb.2022.109894>, URL <https://www.sciencedirect.com/science/article/pii/S1359836822002736>.
- [5] Yang H, Wang B, Ma L. Designing hierarchical metamaterials by topology analysis with tailored Poisson's ratio and Young's modulus. *Compos Struct* 2019;214:359–78. <http://dx.doi.org/10.1016/j.compstruct.2019.01.076>, URL <https://www.sciencedirect.com/science/article/pii/S0263822318335396>.
- [6] Han Y, Lu W. Evolutionary design of nonuniform cellular structures with optimized Poisson's ratio distribution. *Mater Des* 2018;141:384–94. <http://dx.doi.org/10.1016/j.matdes.2017.12.047>, URL <https://www.sciencedirect.com/science/article/pii/S0264127517311619>.
- [7] Al-Ketan O, Adel Assad M, Abu Al-Rub RK. Mechanical properties of periodic interpenetrating phase composites with novel architected microstructures. *Compos Struct* 2017;176:9–19. <http://dx.doi.org/10.1016/j.compstruct.2017.05.026>, URL <https://www.sciencedirect.com/science/article/pii/S0263822316323157>.
- [8] Mahatme C, Giri J, Chadge R, Bhagat A. Comparative analysis of different lattice topologies for cellular structure optimization in additive manufacturing. *Mater Today: Proc* 2022;62:1591–5. <http://dx.doi.org/10.1016/j.matpr.2022.03.280>, URL <https://www.sciencedirect.com/science/article/pii/S2214785322016170>, International Conference on Recent Advances in Modelling and Simulations Techniques in Engineering and Science.
- [9] Almesmari A, Alagha AN, Naji MM, Sheikh-Ahmad J, Jarrar F. Recent advancements in design optimization of lattice-structured materials. *Adv Energy Mater* 2023;25(17). <http://dx.doi.org/10.1002/adem.202201780>.
- [10] Ufodike CO, Wang H, Ahmed MF, Dolzyk G, Jung S. Design and modeling of bamboo biomorphic structure for in-plane energy absorption improvement. *Mater Des* 2021;205:109736. <http://dx.doi.org/10.1016/j.matdes.2021.109736>, URL <https://www.sciencedirect.com/science/article/pii/S0264127521002896>.
- [11] Limmahakun S, Oloyede A, Sithiseripratip K, Xiao Y, Yan C. 3D-printed cellular structures for bone biomimetic implants. *Addit Manuf* 2017;15:93–101. <http://dx.doi.org/10.1016/j.addma.2017.03.010>, URL <https://www.sciencedirect.com/science/article/pii/S2214860416301865>.
- [12] Tabatabaei M, Atluri SN. Simple and efficient analyses of micro-architected cellular elastic-plastic materials with tubular members. *Int J Plast* 2017;99:186–220. <http://dx.doi.org/10.1016/j.ijplas.2017.09.007>, URL <https://www.sciencedirect.com/science/article/pii/S0749641917303236>.
- [13] Tan C, Zou J, Li S, Jamshidi P, Abena A, Forsey A, Moat RJ, Essa K, Wang M, Zhou K, Attallah MM. Additive manufacturing of bio-inspired multi-scale hierarchically strengthened lattice structures. *Int J Mach Tools Manuf* 2021;167:103764. <http://dx.doi.org/10.1016/j.ijmactools.2021.103764>, URL <https://www.sciencedirect.com/science/article/pii/S0890695521000730>.
- [14] Oliveira PR, May M, Panzera TH, Hiermaier S. Bio-based/green sandwich structures: A review. *Thin-Walled Struct* 2022;177:109426. <http://dx.doi.org/10.1016/j.tws.2022.109426>, URL <https://www.sciencedirect.com/science/article/pii/S0263823122002956>.
- [15] Hou S, Li T, Jia Z, Wang L. Mechanical properties of sandwich composites with 3d-printed auxetic and non-auxetic lattice cores under low velocity impact. *Mater Des* 2018;160:1305–21. <http://dx.doi.org/10.1016/j.matdes.2018.11.002>, URL <https://www.sciencedirect.com/science/article/pii/S0264127518308086>.
- [16] Ghannadpour S, Mahmoudi M, Hossein Nedjad K. Structural behavior of 3D-printed sandwich beams with strut-based lattice core: Experimental and numerical study. *Compos Struct* 2022;281:115113. <http://dx.doi.org/10.1016/j.compstruct.2021.115113>, URL <https://www.sciencedirect.com/science/article/pii/S0263822321015312>.
- [17] Chang L, Shen X, Dai Y, Wang T, Zhang L. Investigation on the mechanical properties of topologically optimized cellular structures for sandwiched morphing skins. *Compos Struct* 2020;250:112555. <http://dx.doi.org/10.1016/j.compstruct.2020.112555>, URL <https://www.sciencedirect.com/science/article/pii/S0263822320302300>.
- [18] Shokri Rad M, Prawoto Y, Ahmad Z. Analytical solution and finite element approach to the 3D re-entrant structures of auxetic materials. *Mech Mater* 2014;74:76–87. <http://dx.doi.org/10.1016/j.mechmat.2014.03.012>, URL <https://www.sciencedirect.com/science/article/pii/S0167663614000556>.

- [19] Wu X, Su Y, Shi J. In-plane impact resistance enhancement with a graded cell-wall angle design for auxetic metamaterials. *Compos Struct* 2020;247:112451. <http://dx.doi.org/10.1016/j.compstruct.2020.112451>, URL <https://www.sciencedirect.com/science/article/pii/S026382231934454X>.
- [20] Logakannan KP, Ramachandran V, Rengaswamy J, Ruan D. Dynamic performance of a 3D Re-entrant structure. *Mech Mater* 2020;148:103503. <http://dx.doi.org/10.1016/j.mechmat.2020.103503>, URL <https://www.sciencedirect.com/science/article/pii/S0167663620305457>.
- [21] Bates SR, Farrow IR, Trask RS. Compressive behaviour of 3D printed thermoplastic polyurethane honeycombs with graded densities. *Mater Des* 2019;162:130–42. <http://dx.doi.org/10.1016/j.matdes.2018.11.019>, URL <https://www.sciencedirect.com/science/article/pii/S0264127518308256>.
- [22] Ejeh CJ, Barsoum I, Abu Al-Rub RK. Flexural properties of functionally graded additively manufactured AlSi10Mg TPMS latticed-beams. *Int J Mech Sci* 2022;223:107293. <http://dx.doi.org/10.1016/j.ijmecsci.2022.107293>, URL <https://www.sciencedirect.com/science/article/pii/S0020740322002089>.
- [23] Wang N, Meenashisundaram GK, Chang S, Fuh JYH, Dheen ST, Senthil Kumar A. A comparative investigation on the mechanical properties and cytotoxicity of cubic, octet, and TPMS gyroid structures fabricated by selective laser melting of stainless steel 316L. *J Mech Behav Biomed Mater* 2022;129:105151. <http://dx.doi.org/10.1016/j.jmbbm.2022.105151>, URL <https://www.sciencedirect.com/science/article/pii/S1751616122000741>.
- [24] Peng C, Tran P, Mouritz AP. Compression and buckling analysis of 3D printed carbon fibre-reinforced polymer cellular composite structures. *Compos Struct* 2022;300:116167. <http://dx.doi.org/10.1016/j.compstruct.2022.116167>, URL <https://www.sciencedirect.com/science/article/pii/S0263822322008996>.
- [25] Zhang H, Lin G, Sun W. Structural design and tunable mechanical properties of novel corrugated 3D lattice metamaterials by geometric tailoring. *Thin-Walled Struct* 2023;184:110495. <http://dx.doi.org/10.1016/j.tws.2022.110495>, URL <https://www.sciencedirect.com/science/article/pii/S0263823122010473>.
- [26] Li J, Zhang Z-Y, Liu H-T, Wang Y-B. Design and characterization of novel bi-directional auxetic cubic and cylindrical metamaterials. *Compos Struct* 2022;299:116015. <http://dx.doi.org/10.1016/j.compstruct.2022.116015>, URL <https://www.sciencedirect.com/science/article/pii/S0263822322007668>.
- [27] Moat R, Muyupa E, Imediegwu C, Clarke D, Jowers I, Grimm U. Compressive behaviour of cellular structures with aperiodic order. *Results Mater* 2022;15:100293. <http://dx.doi.org/10.1016/j.rinma.2022.100293>, URL <https://www.sciencedirect.com/science/article/pii/S2590048X22000413>.
- [28] Chen G, Cheng Y, Zhang P, Cai S, Liu J. Blast resistance of metallic double arrowhead honeycomb sandwich panels with different core configurations under the paper tube-guided air blast loading. *Int J Mech Sci* 2021;201:106457. <http://dx.doi.org/10.1016/j.ijmecsci.2021.106457>, URL <https://www.sciencedirect.com/science/article/pii/S0020740321001922>.
- [29] Lu Q, Qi D, Li Y, Xiao D, Wu W. Impact energy absorption performances of ordinary and hierarchical chiral structures. *Thin-Walled Struct* 2019;140:495–505. <http://dx.doi.org/10.1016/j.tws.2019.04.008>, URL <https://www.sciencedirect.com/science/article/pii/S0263823118314538>.
- [30] Andrew JJ, Alhashmi H, Schiffer A, Kumar S, Deshpande VS. Energy absorption and self-sensing performance of 3D printed CF/PEEK cellular composites. *Mater Des* 2021;208:109863. <http://dx.doi.org/10.1016/j.matdes.2021.109863>, URL <https://www.sciencedirect.com/science/article/pii/S0264127521004160>.
- [31] Shukla S, Behera B. Auxetic fibrous structures and their composites: A review. *Compos Struct* 2022;290:115530. <http://dx.doi.org/10.1016/j.compstruct.2022.115530>, URL <https://www.sciencedirect.com/science/article/pii/S0263822322003208>.
- [32] Zhang X, Zhang K, Zhang L, Wang W, Li Y, He R. Additive manufacturing of cellular ceramic structures: From structure to structure–function integration. *Mater Des* 2022;215:110470. <http://dx.doi.org/10.1016/j.matdes.2022.110470>, URL <https://www.sciencedirect.com/science/article/pii/S0264127522000910>.
- [33] Reyes RL, Ghim M-S, Kang N-U, Park J-W, Gwak S-J, Cho Y-S. Development and assessment of modified-honeycomb-structure scaffold for bone tissue engineering. *Addit Manuf* 2022;54:102740. <http://dx.doi.org/10.1016/j.addma.2022.102740>, URL <https://www.sciencedirect.com/science/article/pii/S2214860422001440>.
- [34] Sala R, Regondi S, Graziosi S, Pugliese R. Insights into the printing parameters and characterization of thermoplastic polyurethane soft triply periodic minimal surface and honeycomb lattices for broadening material extrusion applicability. *Addit Manuf* 2022;58:102976. <http://dx.doi.org/10.1016/j.addma.2022.102976>, URL <https://www.sciencedirect.com/science/article/pii/S2214860422003694>.
- [35] Xu M, Zhao Z, Wang P, Duan S, Lei H, Fang D. Mechanical performance of bio-inspired hierarchical honeycomb metamaterials. *Int J Solids Struct* 2022;254–255:111866. <http://dx.doi.org/10.1016/j.ijsoistr.2022.111866>, URL <https://www.sciencedirect.com/science/article/pii/S0020768322003341>.
- [36] Wang Z, Lei Z, Li Z, Yuan K, Wang X. Mechanical reinforcement mechanism of a hierarchical Kagome honeycomb. *Thin-Walled Struct* 2021;167:108235. <http://dx.doi.org/10.1016/j.tws.2021.108235>, URL <https://www.sciencedirect.com/science/article/pii/S0263823121004730>.
- [37] Dou H, Ye W, Zhang D, Cheng Y, Wu C. Comparative study on in-plane compression properties of 3D printed continuous carbon fiber reinforced composite honeycomb and aluminum alloy honeycomb. *Thin-Walled Struct* 2022;176:109335. <http://dx.doi.org/10.1016/j.tws.2022.109335>, URL <https://www.sciencedirect.com/science/article/pii/S0263823122002464>.
- [38] Ahalya Kumar K, Krishnan BR, Venkata Siva Prasad K, Rama Sreekanth P. Comparative study of inplane gradient cellular pattern honeycombs with uniform compliant honeycombs. *Mater Today: Proc* 2022;56:1575–81. <http://dx.doi.org/10.1016/j.matpr.2021.11.657>, URL <https://www.sciencedirect.com/science/article/pii/S2214785322003583>, First International Conference on Advances in Mechanical Engineering and Material Science.
- [39] J JA, Schneider J, Schiffer A, Hafeez F, Kumar S. Dynamic crushing of tailored honeycombs realized via additive manufacturing. *Int J Mech Sci* 2022;219:107126. <http://dx.doi.org/10.1016/j.ijmecsci.2022.107126>, URL <https://www.sciencedirect.com/science/article/pii/S0020740322000583>.
- [40] Abayazid FF, Carpanen D, Ghajari M. New viscoelastic circular cell honeycombs for controlling shear and compressive responses in oblique impacts. *Int J Mech Sci* 2022;222:107262. <http://dx.doi.org/10.1016/j.ijmecsci.2022.107262>, URL <https://www.sciencedirect.com/science/article/pii/S0020740322001813>.
- [41] Zeng C, Liu L, Bian W, Leng J, Liu Y. Compression behavior and energy absorption of 3D printed continuous fiber reinforced composite honeycomb structures with shape memory effects. *Addit Manuf* 2021;38:101842. <http://dx.doi.org/10.1016/j.addma.2021.101842>, URL <https://www.sciencedirect.com/science/article/pii/S2214860421000075>.
- [42] Hu B, Li M, Jiang J, Zhai W. Development of microcellular thermoplastic polyurethane honeycombs with tailored elasticity and energy absorption via CO2 foaming. *Int J Mech Sci* 2021;197:106324. <http://dx.doi.org/10.1016/j.ijmecsci.2021.106324>, URL <https://www.sciencedirect.com/science/article/pii/S002074032100059X>.
- [43] Zhang J, Lu G, You Z. Large deformation and energy absorption of additively manufactured auxetic materials and structures: A review. *Composites B* 2020;201:108340. <http://dx.doi.org/10.1016/j.compositesb.2020.108340>, URL <https://www.sciencedirect.com/science/article/pii/S1359836820333898>.
- [44] Novak N, Biasetto L, Rebesan P, Zanini F, Carmignato S, Krstulović-Opara L, Vesenjak M, Ren Z. Experimental and computational evaluation of tensile properties of additively manufactured hexa- and tetrahedral auxetic cellular structures. *Addit Manuf* 2021;45:102022. <http://dx.doi.org/10.1016/j.addma.2021.102022>, URL <https://www.sciencedirect.com/science/article/pii/S2214860421001871>.
- [45] Najafi M, Ahmadi H, Liaghat G. Experimental investigation on energy absorption of auxetic structures. *Mater Today: Proc* 2021;34:350–5. <http://dx.doi.org/10.1016/j.matpr.2020.06.075>, URL <https://www.sciencedirect.com/science/article/pii/S2214785320345223>, 12th International Conference on Composite Science and Technology.
- [46] Yang H, Ma L. Design and characterization of axisymmetric auxetic metamaterials. *Compos Struct* 2020;249:112560. <http://dx.doi.org/10.1016/j.compstruct.2020.112560>, URL <https://www.sciencedirect.com/science/article/pii/S0263822320313131>.
- [47] Zhang X, Hao H, Tian R, Xue Q, Guan H, Yang X. Quasi-static compression and dynamic crushing behaviors of novel hybrid re-entrant auxetic metamaterials with enhanced energy-absorption. *Compos Struct* 2022;288:115399. <http://dx.doi.org/10.1016/j.compstruct.2022.115399>, URL <https://www.sciencedirect.com/science/article/pii/S0263822322001994>.
- [48] Wei L, Zhao X, Yu Q, Zhu G. Quasi-static axial compressive properties and energy absorption of star-triangular auxetic honeycomb. *Compos Struct* 2021;267:113850. <http://dx.doi.org/10.1016/j.compstruct.2021.113850>, URL <https://www.sciencedirect.com/science/article/pii/S0263822321003111>.
- [49] Niknam H, Yazdani Sarvestani H, Jakubinek M, Ashrafi B, Akbarzadeh A. 3D printed accordion-like materials: A design route to achieve ultrastretchability. *Addit Manuf* 2020;34:101215. <http://dx.doi.org/10.1016/j.addma.2020.101215>, URL <https://www.sciencedirect.com/science/article/pii/S221486042030587X>.
- [50] Guo M-F, Yang H, Ma L. 3D lightweight double arrow-head lattice auxetic structures with enhanced stiffness and energy absorption performance. *Compos Struct* 2022;290:115484. <http://dx.doi.org/10.1016/j.compstruct.2022.115484>, URL <https://www.sciencedirect.com/science/article/pii/S0263822322002756>.
- [51] Gao Q, Ding Z, Liao W-H. Effective elastic properties of irregular auxetic structures. *Compos Struct* 2022;287:115269. <http://dx.doi.org/10.1016/j.compstruct.2022.115269>, URL <https://www.sciencedirect.com/science/article/pii/S0263822322000800>.
- [52] Wang S, Deng C, Ojo O, Akinrinlola B, Kozub J, Wu N. Design and modeling of a novel three dimensional auxetic reentrant honeycomb structure for energy absorption. *Compos Struct* 2022;280:114882. <http://dx.doi.org/10.1016/j.compstruct.2021.114882>, URL <https://www.sciencedirect.com/science/article/pii/S0263822321013210>.
- [53] Günaydin K, Rea C, Kazancı Z. Energy absorption enhancement of additively manufactured hexagonal and re-entrant (auxetic) lattice structures by using multi-material reinforcements. *Addit Manuf* 2022;59:103076. <http://dx.doi.org/10.1016/j.addma.2022.103076>, URL <https://www.sciencedirect.com/science/article/pii/S2214860422004675>.
- [54] Lakes R. Foam structures with a negative Poisson's ratio. *Science* 1987;235(4792):1038–40. <http://dx.doi.org/10.1126/science.235.4792.1038>, arXiv:https://www.science.org/doi/pdf/10.1126/science.235.4792.1038, URL <https://www.science.org/doi/abs/10.1126/science.235.4792.1038>.
- [55] Wojciechowski K. Constant thermodynamic tension Monte Carlo studies of elastic properties of a two-dimensional system of hard cyclic hexamers. *Mol Phys* 1987;61(5):1247–58. <http://dx.doi.org/10.1080/00268978700101761>, arXiv:https://doi.org/10.1080/00268978700101761.

- [56] Evans KE. Tensile network microstructures exhibiting negative Poisson's ratios. *J Phys D: Appl Phys* 1989;22(12):1870–6. <http://dx.doi.org/10.1088/0022-3727/22/12/011>.
- [57] Yang L, Harrysson O, West H, Cormier D. Mechanical properties of 3D re-entrant honeycomb auxetic structures realized via additive manufacturing. *Int J Solids Struct* 2015;69–70:475–90. <http://dx.doi.org/10.1016/j.ijsolstr.2015.05.005>, URL <https://www.sciencedirect.com/science/article/pii/S0020768315002152>.
- [58] Wang X-T, Li X-W, Ma L. Interlocking assembled 3D auxetic cellular structures. *Mater Des* 2016;99:467–76. <http://dx.doi.org/10.1016/j.matdes.2016.03.088>, URL <https://www.sciencedirect.com/science/article/pii/S0264127516303719>.
- [59] Zhang XY, Ren X, Zhang Y, Xie YM. A novel auxetic metamaterial with enhanced mechanical properties and tunable auxeticity. *Thin-Walled Struct* 2022;174:109162. <http://dx.doi.org/10.1016/j.tws.2022.109162>, URL <https://www.sciencedirect.com/science/article/pii/S0263823122001501>.
- [60] Almesmari A, Baghous N, Ejeh CJ, Barsoum I, Abu Al-Rub RK. Review of additively manufactured polymeric metamaterials: Design, fabrication, testing and modeling. *Polymers* 2023;15(19):3858. <http://dx.doi.org/10.3390/polym15193858>.
- [61] Kadum Njim E, Emad S, Noori Hamzah M. A recent review of the sandwich-structured composite metamaterials: static and dynamic analysis. *J Tek* 2023;85(5):133–49. <http://dx.doi.org/10.11113/jurnalteknologi.v85.20282>.
- [62] Zamani MH, Heidari-Rarani M, Torabi K. Optimal design of a novel graded auxetic honeycomb core for sandwich beams under bending using digital image correlation (DIC). *Compos Struct* 2022;286:115310. <http://dx.doi.org/10.1016/j.compstruct.2022.115310>, URL <https://www.sciencedirect.com/science/article/pii/S0263822322001179>.
- [63] Ingrole A, Hao A, Liang R. Design and modeling of auxetic and hybrid honeycomb structures for in-plane property enhancement. *Mater Des* 2017;117:72–83. <http://dx.doi.org/10.1016/j.matdes.2016.12.067>, URL <https://www.sciencedirect.com/science/article/pii/S0264127516315921>.
- [64] Zhang XG, Ren X, Jiang W, Zhang XY, Luo C, Zhang Y, Xie YM. A novel auxetic chiral lattice composite: Experimental and numerical study. *Compos Struct* 2022;282:115043. <http://dx.doi.org/10.1016/j.compstruct.2021.115043>, URL <https://www.sciencedirect.com/science/article/pii/S026382232101463X>.
- [65] Zhang H, Chen P, Zhang Z, Lin G, Sun W. Structural response and energy absorption assessment of corrugated wall mechanical metamaterials under static and dynamic compressive loading. *Int J Impact Eng* 2023;172:104427. <http://dx.doi.org/10.1016/j.ijimpeng.2022.104427>, URL <https://www.sciencedirect.com/science/article/pii/S0734743X22002676>.
- [66] Zhang H, Sun W. Mechanical behavior and crashworthiness assessment of corrugated inner rib reinforced tubular structures. *Thin-Walled Struct* 2023;189:110894. <http://dx.doi.org/10.1016/j.tws.2023.110894>, URL <https://www.sciencedirect.com/science/article/pii/S0263823123003725>.
- [67] Choudhry NK, Panda B, Kumar S. In-plane energy absorption characteristics of a modified re-entrant auxetic structure fabricated via 3D printing. *Composites B* 2022;228:109437. <http://dx.doi.org/10.1016/j.compositesb.2021.109437>, URL <https://www.sciencedirect.com/science/article/pii/S1359836821008052>.
- [68] Shen J, Liu K, Zeng Q, Ge J, Dong Z, Liang J. Design and mechanical property studies of 3D re-entrant lattice auxetic structure. *Aerosp Sci Technol* 2021;118:106998. <http://dx.doi.org/10.1016/j.ast.2021.106998>, URL <https://www.sciencedirect.com/science/article/pii/S1270963821005083>.
- [69] Xu F, Yu K, Hua L. In-plane dynamic response and multi-objective optimization of negative Poisson's ratio (NPR) honeycomb structures with sinusoidal curve. *Compos Struct* 2021;269:114018. <http://dx.doi.org/10.1016/j.compstruct.2021.114018>, URL <https://www.sciencedirect.com/science/article/pii/S0263822321004785>.
- [70] Valle R, Pincheira G, Tuninetti V. Design of an auxetic cellular structure with different elastic properties in its three orthogonal directions. *Proc Inst Mech Eng L* 2021;235(6):1341–50. <http://dx.doi.org/10.1177/14644207211010209>, arXiv: <https://doi.org/10.1177/14644207211010209>.
- [71] Valle R, Pincheira G, Tuninetti V, Fernandez E, Uribe-Lam E. Design and characterization of asymmetric cell structure of auxetic material for predictable directional mechanical response. *Materials* 2022;15(5):1841. <http://dx.doi.org/10.3390/ma15051841>.
- [72] Yang L, Cormier D, West H, Harrysson O, Knowlson K. Non-stochastic Ti–6Al–4V foam structures with negative Poisson's ratio. *Mater Sci Eng A* 2012;558:579–85. <http://dx.doi.org/10.1016/j.msea.2012.08.053>.
- [73] Yang L, Harrysson O, West H, Cormier D. Compressive properties of Ti–6Al–4V auxetic mesh structures made by electron beam melting. *Acta Mater* 2012;60(8):3370–9. <http://dx.doi.org/10.1016/j.actamat.2012.03.015>, URL <https://www.sciencedirect.com/science/article/pii/S1359645412001954>.
- [74] Valle R, Pincheira G, Tuninetti V, Garrido C, Treviño C, Morales J. Evaluation of the orthotropic behavior in an auxetic structure based on a novel design parameter of a square cell with re-entrant struts. *Polymers* 2022;14(20). <http://dx.doi.org/10.3390/polym14204325>, URL <https://www.mdpi.com/2073-4360/14/20/4325>.
- [75] Zhang X-c, Ding H-m, An L-q, Wang X-l. Numerical investigation on dynamic crushing behavior of auxetic honeycombs with various cell-wall angles. *Adv Mech Eng* 2014;7:679678. <http://dx.doi.org/10.1155/2014/679678>.
- [76] Andrews E, Gibson LJ, Ashby M. The creep of cellular solids. *Acta Mater* 1999;47(10):2853–63.
- [77] Li Z, Fan J, Wang Z, Zhao L. On crushing response of the three-dimensional closed-cell foam based on Voronoi model. *Mech Mater* 2014;68:85–94. <http://dx.doi.org/10.1016/j.mechmat.2013.08.009>.
- [78] Chen Y, Jia L, Liu C, Zhang Z, Ma L, Chen C, Banthia N, Zhang Y. Mechanical anisotropy evolution of 3D-printed alkali-activated materials with different GGBFS/FA combinations. *J Build Eng* 2022;50:104126. <http://dx.doi.org/10.1016/j.jobbe.2022.104126>, URL <https://www.sciencedirect.com/science/article/pii/S2352710222001395>.
- [79] Vangelatos Z, Komvopoulos K, Spanos J, Farsari M, Grigoropoulos C. Anisotropic and curved lattice members enhance the structural integrity and mechanical performance of architected metamaterials. *Int J Solids Struct* 2020;193–194:287–301. <http://dx.doi.org/10.1016/j.ijsolstr.2020.02.023>, URL <https://www.sciencedirect.com/science/article/pii/S0020768320300640>.
- [80] Maskery I, Aboulkhair N, Aremu A, Tuck C, Ashcroft I. Compressive failure modes and energy absorption in additively manufactured double gyroid lattices. *Addit Manuf* 2017;16:24–9. <http://dx.doi.org/10.1016/j.addma.2017.04.003>, URL <https://www.sciencedirect.com/science/article/pii/S2214860417301203>.
- [81] Pagliocca N, Youssef G, Koohbor B. In-plane mechanical and failure responses of honeycombs with syntactic foam cell walls. *Compos Struct* 2022;295:115866. <http://dx.doi.org/10.1016/j.compstruct.2022.115866>, URL <https://www.sciencedirect.com/science/article/pii/S026382232200633X>.
- [82] Maskery I, Aboulkhair N, Aremu A, Tuck C, Ashcroft I, Wildman R, Hague R. A mechanical property evaluation of graded density Al–Si10–Mg lattice structures manufactured by selective laser melting. *Mater Sci Eng A* 2016;670:264–74. <http://dx.doi.org/10.1016/j.msea.2016.06.013>, URL <https://www.sciencedirect.com/science/article/pii/S092150931630658X>.